Proceedings of ICMEM2005
International Conference on Mechanical Engineering and Mechanics
October 26-28, 2005, Nanjing, China

Hydroelastic Analysis of Flexible Floating Structures in Regular Waves

Xujun Chen[1,2,3], Torgeir Moan[2], Shixiao Fu[2], Weicheng Cui [3]
1 Engineering Institute of Engineering Corps, PLA University of Science and Technology, Nanjing 210007, China
2 Centre for Ships and Ocean Structures, Norwegian University of Science and Technology, N-7491, Trondheim, Norway
3 China Ship Scientific Research Center, Wuxi 214082, China
E-mail: xjchen@sjtu.edu.cn

Abstract: Linear hydroelasticity is introduced to investigate the hydroelastic responses of flexible floating structures to regular waves in the frequency domain. The fluid around the floating models is assumed to be ideal and its behaviour is modelled by velocity potentials. The controlling equations are solved with Green Function method under relevant boundary conditions at the free surface condition, fixed hull surface condition, deep-water condition and far field radiation condition. Two models are used as numerical examples. Experimental results are compared with numerical results (such as the principal responses, vertical displacement of different points to different incident wave circular frequencies, etc.). Fore-and-aft of the models have different maximum vertical displacements to a given incident wave. When the incident wave frequencies are close to the wet natural frequencies of the flexible modes, the vibrations or relatively large responses are found, and these modes will have a great influence on the total displacement responses

Keywords: Hydroelasticity; VLFS; Flexible connector

1 Introduction

For a flexible floating structure, such as a very large floating structure (VLFS)[1-4] or a structure composed of several floaters connected by flexible connectors [5], structural responses of the body should not be obtained by the classical rigid body sea keeping analysis. Rather it is necessary to account for the direct hydroelastic coupling behaviour of fluid and structures. Linear hydroelastic theories [6,7] have been applied to the design and research related to marine structures for several decades. Also nonlinear procedures [8-10] are increasingly applied.

By using the three-dimensional linear hydroelasticity theory proposed by Wu [7], two flexible floating laboratory models are analysed in this paper. The first flexible floating model consisted of 12 floaters interconnected by means of two elastic plates [5]. The length, width and height of each floater are respectively 0.19m, 0.6m and 0.25m, and the two elastic plates are made of steel. The second one is a VLFS[11]. With a full scale, the length, width and height of the model are 300m, 60m and 2m respectively. The numerical results are compared with the experimental ones, and good agreement is found, especially for the one of the VLFS model.

2 Basic Theory

The fluid around the flexible floating body is assumed to be ideal (i.e. uniform, continuous, inviscid, incompressible and irrotational) and the surface wave is of small amplitude. Hence, the fluid behaviour can be fully governed by the velocity potential. In order to simplify the expression, two coordinate systems are introduced, namely the equilibrium frame of $Oxyz$, and the body fixed axes system $O'x'y'z'$. The origin of the $Oxyz$ system is on the point of the intersection of the steady water surface and the vertical line, which goes through the gravity centre of the structure, and the axis *Oz* is upward. The $O'x'y'z'$ system is fixed on the floating body.

2.1 Decomposition of the velocity potential and hydrodynamic forces

Based on the assumptions of the fluid field, the velocity potential (unsteady velocity potential) around the floating body in the equilibrium frame may be decomposed into the form (see e.g. [7])

$$\phi(x,y,z,t)=\phi_I+\phi_D+\sum_{r=1}^{m}\phi_r\ , \tag{1}$$

where $\phi_I(x,y,z,t)$, $\phi_D(x,y,z,t)$ and $\phi_r(x,y,z,t)$ denote the incident wave potential, diffraction wave potential, and radiation wave potential arising from the responses of the flexible body. In frequency domain, the unsteady velocity potential and the vibration principal coordinates may be further expressed as

$$\phi=\mathrm{Re}\left\{\left[\varphi_I+\varphi_D+\sum_{r=1}^{m}\varphi_r p_r\right]\mathrm{e}^{\mathrm{i}\omega t}\right\}, \tag{2}$$

$$p_r(t)=\mathrm{Re}\left\{p_r\,\mathrm{e}^{\mathrm{i}\omega t}\right\}, \tag{3}$$

where ω is the wave circular frequency; $\varphi_I(x,y,z,\omega)$ and $\varphi_D(x,y,z,\omega)$ are components of the incident wave velocity potential and the diffraction wave potential respectively; $\varphi_r(x,y,z,\omega)$ $(r=1,\cdots,m)$ is the components of the radiation wave potential arising from the vibration in the r-th principal dry mode of the flexible body, with unit amplitude and frequency is ω; m is the number of modes; $p_r(\omega)$ is the complex amplitude of the principal coordinate. The sign Re{ } in Equations (2) and (3) denotes the real part of the complex in { }. The sign Re{ } is omitted in the following expressions of the potentials and the principal coordinates for clarity. With a given wave circular frequency ω, $\varphi_D(x,y,z,\omega)$ and $\varphi_r(x,y,z,\omega)$ can be solved by the Green Function Method [12] under the following governing equation and boundary conditions.

$$\begin{cases} [\Omega]: & \nabla^2\varphi_v = 0 \\ [\mathrm{S_F}]: & g\dfrac{\partial\varphi_v}{\partial z} - \omega^2\varphi_v = 0 \\ [\mathrm{S}\ ]: & \dfrac{\partial\varphi_D}{\partial n} = -\dfrac{\partial\varphi_I}{\partial n},\quad \dfrac{\partial\varphi_r}{\partial n} = -\mathrm{i}\,\omega\vec{u}_r^{\,0}\vec{n} \\ [\mathrm{S_B}]: & \dfrac{\partial\varphi_v}{\partial z} = 0 \\ [\mathrm{S}_\infty]: & \varphi_v \to 0 \end{cases} \quad (4)$$

where $[\Omega]$, $[\mathrm{S_F}]$, $[\mathrm{S}\ ]$, $[\mathrm{S_B}]$ and $[\mathrm{S}_\infty]$ mean the fluid field, the free surface, the hull surface, the sea bed and the far field cylinder respectively; $\vec{n}$ denotes the normal vectors of the body's wetted surface defined in $Oxyz$; g is the gravity acceleration; $\vec{u}_r^{\,0}$ denotes the r-th mode of the structure in vacuum, it can be obtained from a structural analysis codes; φ_v can be φ_D or φ_r. The Lagrange integral equation gives the relationship between the velocity potential and the pressure of the fluid as

$$\frac{p(x,y,z,t)}{\rho} + gz + \frac{\partial\phi}{\partial t} = 0. \quad (5)$$

$p(x,y,z,t)$ and ρ are respectively the pressure and the density of the fluid.

The fluid pressure acting on the mean wetted surface $\bar{S}$ during the motion and distortion of the body is given by the Bernoulli equation in the equilibrium axes system,

$$p(x,y,z,t)\big|_{\bar{S}} = -\rho\left(\frac{\partial\phi}{\partial t} + gz\right)_{\bar{S}}. \quad (6)$$

The generalized forces acted on the floating body can be expressed as

$$Z_r(t) = -\iint_{\bar{S}} \vec{n}\cdot\vec{u}_r^{\,0}\, p\,\mathrm{d}S. \quad (7)$$

Substitution of Equations (2) and (6) into Equation (7) yields

$$Z_r(t) = Z_r^{(0)} + E_r(t) + H_r(t) + R_r(t), \quad (8)$$

where $Z_r^{(0)}$, $E_r(t)$, $H_r(t)$ and $R_r(t)$ are the generalized constant forces, the generalized wave exciting forces, radiation forces and restoring forces. They are be respectively expressed as follows:

$$Z_r^{(0)} = \rho\iint_{\bar{S}} \vec{n}\cdot\vec{u}_r^{\,0} gz'\,\mathrm{d}S, \quad (9)$$

$$\begin{aligned} E_r(t) &= \rho\iint_{\bar{S}} \vec{n}\cdot\vec{u}_r^{\,0}\frac{\partial}{\partial t}[\phi_I(t) + \phi_D(t)]\,\mathrm{d}S \\ &= \xi_r(\omega)\mathrm{e}^{\mathrm{i}\omega t} \end{aligned}, \quad (10)$$

$$\begin{aligned} H_r(t) &= \sum_{k=1}^{m}\rho\iint_{\bar{S}} \vec{n}\cdot\vec{u}_r^{\,0}\frac{\partial}{\partial t}\phi_k(t)\,\mathrm{d}S \\ &= \sum_{k=1}^{m}\left[\omega^2 A_{rk}(\omega) - \mathrm{i}\,\omega B_{rk}(\omega)\right]p_k(\omega)\mathrm{e}^{\mathrm{i}\omega t} \end{aligned}, \quad (11)$$

$$R_r(t) = \rho\iint_{\bar{S}} \vec{n}\cdot\vec{u}_r^{\,0} gw\,\mathrm{d}S = \sum_{k=1}^{m} C_{rk}\,p_k(\omega)\mathrm{e}^{\mathrm{i}\omega t}, \quad (12)$$

where

$$\xi_r(\omega) = \rho\iint_{\bar{S}} \vec{n}\cdot\vec{u}_r^{\,0}(\mathrm{i}\,\omega)[\varphi_I(\omega) + \varphi_D(\omega)]\,\mathrm{d}S, \quad (13)$$

$$\begin{cases} A_{rk}(\omega) = \dfrac{1}{\omega^2}\mathrm{Re}\left\{\mathrm{i}\,\rho\iint_{\bar{S}} \vec{n}\cdot\vec{u}_r^{\,0}\,\omega\varphi_k(\omega)\,\mathrm{d}S\right\}, \\ B_{rk}(\omega) = \dfrac{\mathrm{i}}{\omega}\mathrm{Im}\left\{\mathrm{i}\,\rho\iint_{\bar{S}} \vec{n}\cdot\vec{u}_r^{\,0}\,\omega\varphi_k(\omega)\,\mathrm{d}S\right\}, \end{cases} \quad (14)$$

$$C_{rk} = \rho\iint_{\bar{S}} \vec{n}\cdot\vec{u}_r^{\,0} gw_k^0\,\mathrm{d}S, \quad (15)$$

are the coefficients of the generalized wave exciting forces, the coefficients of added mass and added damping, and the frequency independent coefficients of the generalized restoring forces. w in Equation (12) and w_k^0 in Equation (15) are vertical displacement and the vertical displacement component of the mode k.

2.2 Equation of motion

Based on the solutions of the generalized fluid forces acting on the flexible floating body, the equations of motion for solving the vibration principal coordinates $p_k(t)$ may be represented as

$$\begin{aligned} &\sum_{k=1}^{m}\left[(a_{rk} + A_{rk})\ddot{p}_k(t) + (b_{rk} + B_{rk})\dot{p}_k(t)\right. \\ &\left.+ (c_{rk} + C_{rk})p_k(t)\right] = E_r(t) \end{aligned}, \quad (16)$$

where a_{rk}, b_{rk} and c_{rk} are the elements of the generalized mass matrix, the generalized damping matrix and the generalized rigid matrix of the structure respectively. Equation (16) can be solved in frequency domain, the solving equation can be expressed as

$$\begin{aligned} &\sum_{k=1}^{m}\left[-\omega^2(a_{rk} + A_{rk}) + (\mathrm{i}\,\omega)(b_{rk} + B_{rk})\right. \\ &\left.+ (c_{rk} + C_{rk})\right]p_k(\omega) = \xi_r(\omega),\quad r = 1,2,\cdots,m \end{aligned}. \quad (17)$$

When the responses of the principal coordinates have been obtained, one can calculate the vertical displacement by using the following equation

$$w(t) = \sum_{r=1}^{m} w_r\,p_r(t), \quad (18)$$

where w_r are the vertical displacement modes of the floating body. w_r as well as a_{rk} and c_{rk} in Equation (17) can obtained directly from relevant structural analysis codes. A structural damping is conveniently introduced by the Rayleigh or proportional damping [13] to form the damping matrix as a linear combination of the stiffness and mass matrices of the structure, that is

$$b_{rr} = \alpha c_{rr} + \beta a_{rr},\qquad r = 7,\cdots,m, \quad (19)$$

where a_{rr} and c_{rr} are diagonal elements of the generalized mass matrix and the generalized rigid matrix respectively; α and β are called, respectively, the stiffness and mass proportional damping constants, which can be associated with the fraction of critical damping ξ as

$$\xi = 0.5(\alpha\omega + \beta/\omega), \tag{20}$$

Therefore, α and β can be determined by choosing the fractions of critical damping (ξ_1 and ξ_2) at two different frequencies (ω_1 and ω_2), and can be solved by the following equations

$$\begin{cases} \alpha = 2(\xi_2\omega_2 - \xi_1\omega_1)/(\omega_2^2 - \omega_1^2), \\ \beta = 2\omega_1\omega_2(\xi_1\omega_2 - \xi_2\omega_1)/(\omega_2^2 - \omega_1^2). \end{cases} \tag{21}$$

In this paper, the Rayleigh damping factors α and β are computed on the basis of the first two natural frequencies ω_1 and ω_2 determined by the damping properties of the dry structure.

3 Example structures

The first flexible floating model (called Model structure 1 in the following text), shown in Figure 1, consisted of 12 floaters interconnected by means of two elastic plates [5]. The length, width and height of each floater are respectively 0.19m, 0.6m and 0.25m, and the two elastic plates are made of steel. The thickness and width of the elastic plates are 4mm and 50mm respectively. The draught of the floater is 0.12m.

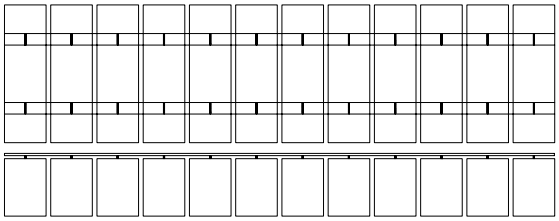

Figure 1 Schematic outline of Model structure 1

The second one is a VLFS [11] (called Structure 2 in the following text). Particulars of the full-scale structure are shown on Table 1.

The natural frequencies and generalised structural damping of the first three vertical bending modes of the two structures are shown in Table 2. Here, we assume that the critical damping ξ_1 and ξ_2 is 5% (The influence of the structural damping will be briefly discussed in the next section).

The mode shapes of the first three vertical bending modes of the Model structure 1 and Structure 2 are shown in Figures 2 and 3 respectively.

Table 1 Particulars of the Structure 2

Particulars	Symbol/Unit	Value
Length	L / m	300.0
Width	B / m	60.0
Height	D / m	2.0
Draught	d / m	0.5
Vertical bending ridigity	EI / Nm^2	4.77×10^{11}
Young's modulus	E / N/m^2	1.19×10^{10}
Poission's ratio	v	0.13
Density	ρ /kg/m^3	256.25

Table 2 Natural frequencies and generalised damping force per unit velocity of the first three vertical bending modes

Mode number	Model structure 1		Structure 2	
	Frequency	GDF/UV*	Frequency	GDF/UV*
1	0.705 Hz	6.334	0.156 Hz	226051
2	1.720 Hz	5.735	0.430 Hz	620418
3	2.960 Hz	8.670	0.845 Hz	18999769

*:GDF/UV means generalised damping force per unit velocity.

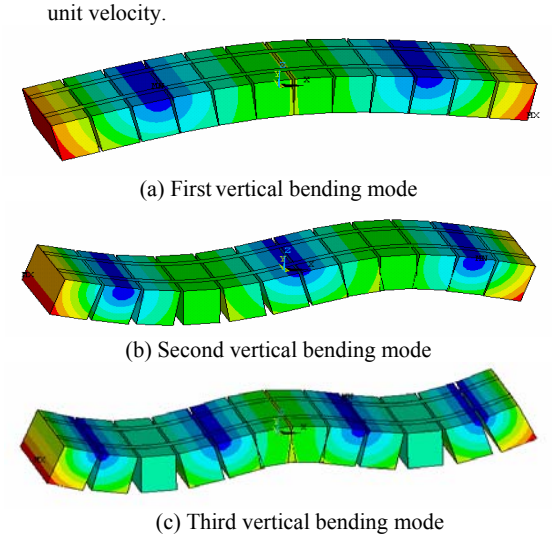

(a) First vertical bending mode

(b) Second vertical bending mode

(c) Third vertical bending mode

Figure 2 First three vertical bending mode shapes of Model structure 1

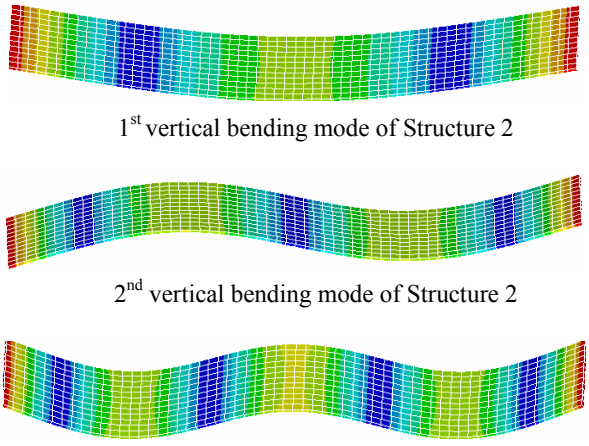

1st vertical bending mode of Structure 2

2nd vertical bending mode of Structure 2

3rd vertical bending mode of Structure 2

Figure 2 First three vertical bending mode shapes of Structure 2

4 Results and Discussion

Figure 4 shows the calculated response amplitude operator (RAO) of the two structures. VB means vertical bending. The pitch response of structure 2 is shown separately in Figure 4(c) for the reason of clarity. A relatively large value of the 1st vertical bending mode can be found in the Figure 4 (a) at the circular frequency of 6.0 rad/s. It is because of this wave exciting frequency is

close to the wet resonance frequency ω_{wr} (=6.01 rad/s) of the first vertical bending mode, which can be calculated by solving the follow characteristic equations [9]

$$-\omega_{wr}^2\left[a_{rr}+A_{rr}(\omega)\right]+\left(c_{rr}+C_{rr}\right)=0. \qquad (22)$$

In Equation (22), $A_{rr}(\omega)$ are diagonal elements of the added mass matrix when the floating body vibrate with the wave frequency ω; a_{rr}, c_{rr} and C_{rr} are diagonal elements of the generalized mass matrix, the rigid matrix and the restoring matrix respectively.

Other resonance phenomena cannot be found in Figure 4. This is because the wet resonant frequencies are larger than 8 rad/s.

Figures 5 and 6 show the vertical displacements of the fore and midship of the two models. The influence of structural damping is shown and compared with the experimental ones of Model structure 1. The agreement of Model 1 is not so good, but that of Structure 2 is very good. It also can be found that the structural damping has a considerable influence on the vertical displacement amplitude of Model structure 1 from the frequency 4rad/s to 6.5rad/s. On the other hand, we found from the calculation results that the influence of the structural damping can be neglected for Structure 2. It is because the natural frequencies of the Structure 2 are very low.

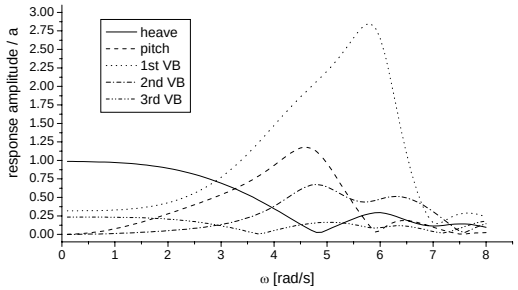

(a) Model structure 1

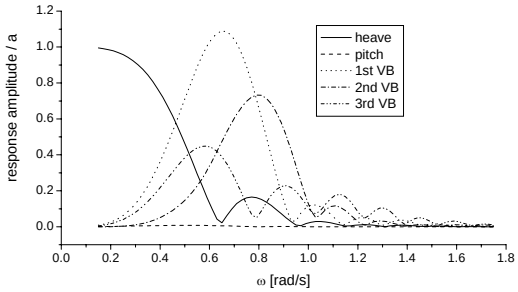

(b) Structure 2

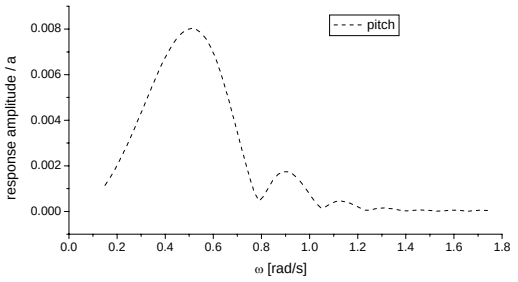

(c) Pitch of structure 2

Figure 4 Relationship between the RAO and the circular frequency

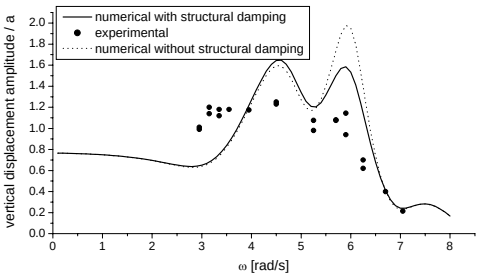

(a) Model structure 1

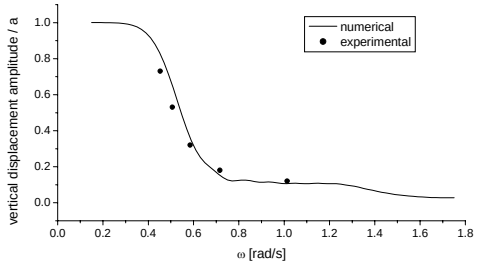

(b) Structure 2

Figure 5 RAO for the vertical displacements of fore part and the circular frequencies

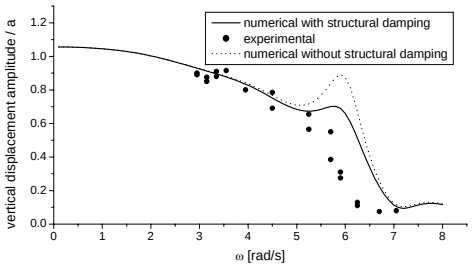

(a) Model structure 1

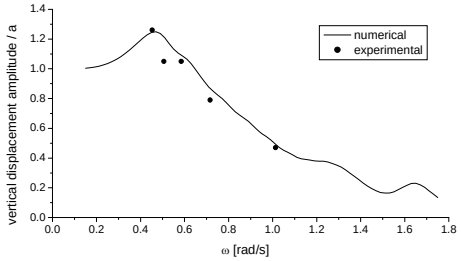

(b) Structure 2

Figure 6 Relationship between the vertical displacements of the midship and the circular frequencies

Figure 7 shows the vertical displacement along the length of the Model 1 for different wavelength, λ. L is the length of the structure. From this figure, it can be found that fore-and-aft of the model have different maximum vertical displacements for a given incident wave. In addition, for short waves, the differences in response along the length of the floating body are bigger than those of long waves.

The wave circular frequencies have a great influence on the vertical displacement. For example, from line 0.8L of Figure 7, it can be found that the pitch mode has great influence on the vertical displacement (implying of the fore and aft are bigger), and also of the first vertical bending modes (implying of the midship is the largest). It is because the frequency corresponding to λ =0.8L is

about 5.6rad/s, which is close to the wet resonance frequencies of pitch (5.7rad/s) and first vertical bending (6.01rad/s).

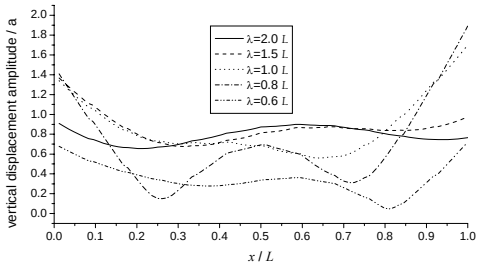

Figure 7 vertical displacements along the length of Model structure 1 for different wavelength, λ

Figure 8 shows the vertical displacement along the length of the structure 2. The results of rigid model as well as the flexible model are shown and compared with the experimental ones. Good agreement is shown between calculation and test results for the flexible model. It is seen that the rigid body model differs significantly from the experimental data. Hence a hydroelastic model is absolutely necessarily for the response analysis of flexible floating structures.

5 Conclusions

The two examples used in this study show the importance of hydroelasticity in analysing flexible floating structures such as a flexible connected floaters or a VLFS.

Resonant characteristics can be found in the analysis when the exciting wave frequency is close to the wet resonance frequency of the floating body.

The displacement varies along the length of the vessel. In general, the response of the fore and aft is relatively larger than that of the midship for short waves. When the wavelength is several times of the length of the floating body, the difference between the ends and midship becomes smaller. This is because the structure follows the wave motion.

Achnowledgement

This word is supported by the National Natural Science Foundation of China (No. 50309018)

References

[1] R C Ertekin, H R Riggs. Proceedings of the First International Workshop on Very Large Floating Structures-VLFS'91. Honolulu, Hawaii, USA, 1991.

[2] Y Watanabe. Proceedings of the Second International Workshop on Very Large Floating Structures-VLFS'96. Hayama, Japan, 1996.

[3] R C Ertekin, H R Riggs. Proceedings of the Third International Workshop on Very Large Floating Structures-VLFS'99, Honolulu, Hawaii, USA, 1999.

[4] Y Watanable. Proceedings of the Third International Workshop on Very Large Floating Structures-VLFS'03, Tokyo, Japan, 2003.

[5] Ŝ Malenica, B Molin, F Remy, I Senjanović. Hydroelastic response of a barge to impulsive and non-impulsive wave loads, the 3rd International Conference on Hydroelasticity in Marine Technology. London, September 2003.

[6] R E D Bishop, W G Price. Hydroelasticity of ships. Cambridge University Press, UK, 1979.

[7] Y S Wu. Hydroelasticity of floating bodies. Ph.D. Thesis, Brunel University. UK, 1984,

[8] J Z Xia, Z H Wang, J J Jensen. Non-linear wave loads and ship responses by a time-domain strip theory. Marine Structure. 1998, 11(3): 101-123

[9] X J Chen, Y S Wu, W C Cui, X F Tang. Nonlinear Hydroelastic Analysis of a Moored Floating Body. Ocean Engineering. 2003, 30(8): 965-1003.

[10] X J Chen, J J Jensen, W C Cui, S X Fu. Hydroelasticity of a Floating Plate in Multi-directional Waves. Ocean Engineering. 2003, 30(15): 1997-2017.

[11] K Yago, H Endo. Model experiment and numerical calculation of the hydroelastic behaviour of matlike VLFS, VLFS'96. Hayama, Japan, 1996:209-214.

[12] J N Newman. Marine Hydrodynamics. the MIT (Massachusetts Institute of Technology) Press. 1986.

[13] J S Wu, P Y Shih. Moving-load-induced vibrations of a moored floating bridge. Computers and Structures. 1998, 66(4): 435-461.

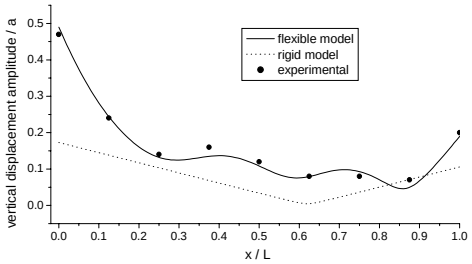

(a) λ / L =0.2

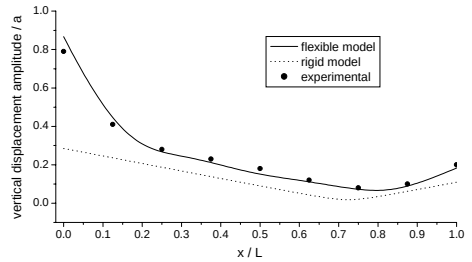

(b) λ / L =0.4

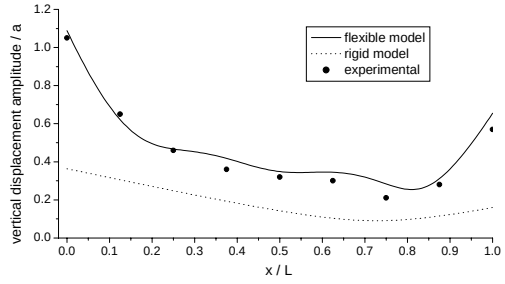

(c) λ / L =0.6

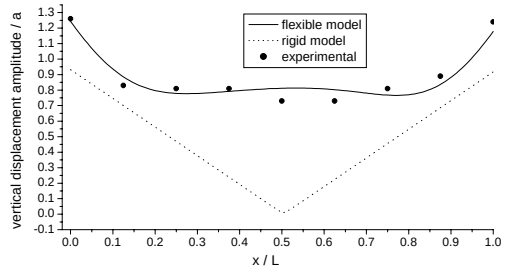

(e) λ / L =1.0

Figure 8 vertical displacements along the length of structure 2